A close and relevant parallel is the ionization of (the isoelectronic) primary amides. Here too calculations indicate that the *Z* isomer (of the anion) is more stable in the gas phase by about 5 kcal/mol.[18] Since the isomeric anions are in equilibrium with the same conjugate acid, this is a direct measure of the difference in acidity between the *E* and *Z* protons. In this case it is possible

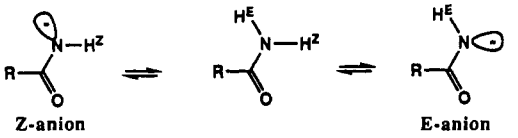

to measure the equilibria, and the proton-transfer processes involved, in solution. In aqueous solvent, the base-catalyzed exchange of H^E is never more than a few times faster than that of H^Z; the *E*/*Z* ratio is strongly solvent-dependent, and under some conditions the solvated *E* isomer is actually preferred.[19]

(17) The calculated (>5 kcal/mol) preference of esters for the *Z* conformation is also much reduced in solution, as indicated by a measured (^{13}C NMR) value of 1.67 kcal/mol for ethyl formate. (Grindley, T. B. *Tetrahedron Lett.* **1982**, 1757-60.) Increasing the size of either the acyl or the alkyl substituent increases the preference for the *Z* conformation, presumably for steric reasons, so any stereoelectronic preference should be most clearly expressed in formate esters.

(18) Zielinski, T. J.; Poirier, R. A.; Peterson, M. R.; Csizmadia, I. G. *J. Comput. Chem.* **1982**, *3*, 477-485. Nguyen, N. T.; Hegarty, A. F. *J. Org. Chem.* **1986**, *51*, 4703-6.

(19) Perrin, C. L.; Johnston, E. R.; Lollo, C. P.; Kobrin, P. A. *J. Am. Chem. Soc.* **1981**, *103*, 4691-6. Perrin, C. L.; Lollo, C. P.; Hahn, C.-S. *J. Org. Chem.* **1986**, *50*, 1405-9.

Kinetic Studies and Modeling of a Self-Replicating System†

James S. Nowick, Qing Feng, Tjama Tjivikua, Pablo Ballester, and Julius Rebek, Jr.*

Contribution from the Department of Chemistry, Massachusetts Institute of Technology, Cambridge, Massachusetts 02139. *Received April 29, 1991*

Abstract: The design, synthesis, and study of a molecular template, **11a**, that catalyzes its own formation from simpler components, **9** and **10d**, is described. Autocatalysis is shown by the following: (1) the increase in rate of reaction of **9** and **10d** in the presence of **11a**; (2) the reduction in rate of reaction in the presence of 2,6-bis(acetylamino)pyridine inhibitor; and (3) the reduction in rate of reaction when a component incapable of template behavior, **10h**, is substituted for **10d**. Three kinetic pathways are elucidated: (1) the background bimolecular reaction (eq 6); (2) the preassociative mechanism (eq 7); and (3) the template termolecular process (eq 8). A kinetic model for the replication process is introduced, and equilibrium and rate constants are determined. Predictions for the shapes of the product growth curves are made.

Introduction

Replicating molecules stand on the boundary of chemistry and biology. Replication itself bears no structural content, yet the process invariably involves molecules that are complementary. This feature is apparent in the structure of double-stranded nucleic acids, and perhaps it is too obvious or self-evident to have warranted much discussion in the past. Whereas complementarity implies the presence of "positive" and "negative" molecules (e.g., strands of nucleic acids), *self-complementarity* transcends the need for a "negative" and thus provides a minimal system for replication. We have used *the principle of self-complementarity* as our polar star in this badly trampled terrain; it gives our structures design, shape, and ultimately, function.[1]

Scheme I provides a two-dimensional example of self-complementarity and geometrically illustrates the minimal requirements of a self-replicating system. The sigmoid line represents the intermolecular contact between the two complementary and identical components. These units can be further broken along the jagged line into two different, yet complementary, pieces. The fusion of these pieces leads to a shape that can act as a template for the assembly of an identical unit. (A three-dimensional case has been described elsewhere.[2]) In this paper, we apply this concept in the context of chemical structures.

A brief time ago, we introduced a synthetic system capable of self-replication.[3] Unlike nucleic acids, replication occurs without the aid of enzymes or ribozymes.[4] In contrast with natural systems and other synthetic self-replicating molecules,[5] the new system involves the formation of an amide bond rather than a phosphate bond in the assembly step. Nevertheless, base-pairing provides the recognition and organization of the reacting components. Here, we report the experimental details of the reactions

Scheme I

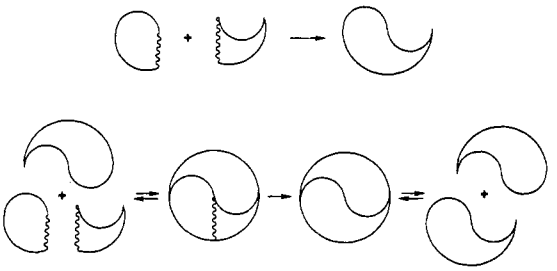

and describe the pecularities of its autocatalytic behavior. In a sequel, we shall address issues concerned with information, growth, and chemical evolution.

Catalysis. One goal of molecular recognition is the merger of the binding and catalytic steps, to make these events converge in space and in time. For the most part, this aim is a restatement of the Pauling principle.[6] It involves the maximum binding to, or recognition of, transition states. The recognition of transition states (rather than, say, their nearby high-energy intermediates) in small model systems is the challenge. Recent progress on this

† Dedicated to Professor George Büchi on the occasion of his 70th birthday.

(1) Rebek, J., Jr. *Angew. Chem., Int. Ed. Engl.* **1990**, *29*, 245-255.
(2) Rebek, J. Jr. *Experientia*, in press.
(3) Tjivikua, T.; Ballester, P.; Rebek, J., Jr. *J. Am. Chem. Soc.* **1990**, *112*, 1249-1250.
(4) (a) Doudna, J. A.; Szostak, J. W. *Nature* **1989**, *339*, 519-522. (b) Doudna, J. A.; Couture, S.; Szostak, J. W. *Science* **1991**, *251*, 1605-1608.
(5) (a) von Kiedrowski, G. *Angew. Chem., Int. Ed. Engl.* **1986**, *25*, 932-935. (b) von Kiedrowski, G.; Wlotzka, B.; Helbing, J. *Angew. Chem., Int. Ed. Engl.* **1989**, *28*, 1235-1237. (c) von Kiedrowski, G.; Wlotzka, B.; Helbing, J.; Mattzen, M.; Jordan, S. *Angew. Chem., Int. Ed. Engl.* **1991**, *30*, 423-426. (d) Zielinski, W. S.; Orgel, L. E. *Nature* **1987**, *327*, 346-347.
(6) Pauling, L. *Chem. Eng. News* **1946**, *24*, 1375-1377.

0002-7863/91/1513-8831$02.50/0

notion involves molecular devices[7] and other machines,[8] catalytic antibodies,[9] and transition state analogue enzyme inhibitors.[10]

Having created synthetic receptors capable of complexing adenine derivatives, we decided to explore the possibility of using the binding step to catalyze a subsequent reaction. The specific intent was to convert an otherwise bimolecular reaction to a unimolecular (intramolecular) one. By understanding how the two components fit together, we could design an arrangement of reacting groups that would lead to a relatively effortless formation of a reactive intermediate within the complex.

The basic binding event in our adenine receptors involves both hydrogen-bonding and aryl-stacking interactions in organic media. The triaxial arrangement of the carboxyl groups of Kemp's triacid **1**[11] provides a U-turn shape and permits the construction of molecules which "fold" back upon themselves. The imide **2a**, which is prepared by condensation of Kemp's triacid with ammonia, presents a hydrogen-bonding edge similar to that of thymine.[12] Aromatic esters and amides of the remaining carboxyl extend beyond the hydrogen-bonding edge, presenting large, polarizable surfaces to guests involved in base-pairing to the edge. Hydrogen-bonding and aromatic-stacking forces *converge from perpendicular directions* to provide a microenvironment complementary to adenine derivatives (eq 1).

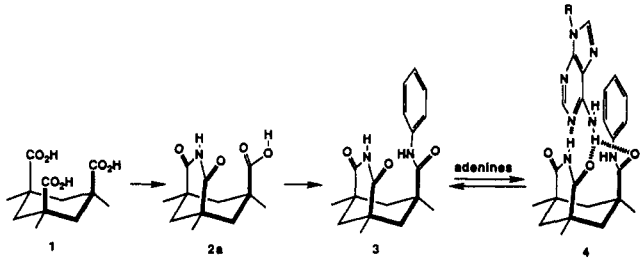

(1)

Mere base-pairing is insufficient to drive two components together in water, so we have used the magnification of hydrogen-bonding forces available in $CHCl_3$ to insure high levels of intermolecular association. In doing so, we also contract the time scale of our experiments to manageable lengths. We attribute the difficulties encountered by previous workers in the field to their use of aqueous media. The effects are so small that only very long times could reveal self-replicating effects at, say, the mononucleotide level.

The intimate contacts featured by these complexes were mapped out by NMR NOE techniques. These provided a level of predictability in the placement of functional groups on the periphery of the components.[12] A roughly 4-fold degeneracy exists in the overall complexation; Watson–Crick and Hoogsteen and reverse Watson–Crick and reverse Hoogsteen base-pairing all contribute to the association. Since some bifurcated hydrogen bonding was detected in the amide derivatives (e.g., **3**),[13] the complexes **4** were regarded as the major contributors. (These represent a complete description when the aromatic group is a phenyl derivative because rotation about the aryl–nitrogen bond does not alter the structure.) With different aromatic surfaces (e.g., the 2-naphthyl), the possibilities of binding are further compounded by the rotational isomerism about the N–aryl bond; this can lead to an actuarial nightmare. For the phenyl derivative, however, groups attached to the 9-position of adenine and the para position of the phenyl were juxtaposed in space. This propinquity eventually led to chemical reactions between the functional groups placed there.

Development of a Self-Replicating System. In designing a molecule that acted as a template for its own formation, we set out to prepare two components bearing *both* complementary reactive-functionality and complementary hydrogen-bonding surfaces. Our first attempts employed the Kemp's triacid imide equipped with a phenyl spacer bearing a para acylating function as an electrophile (**5a**) and 9-(3-aminopropyl)adenine as a nucleophile.[14] The latter was readily available from the alkylation of adenine. Its coupling with the *p*-nitrophenyl ester went smoothly. Competitive inhibition experiments indicated that coupling proceeded by way of the base-paired complex. Addition of other adenine derivatives or 2,6-bis(acetylamino)pyridine to the reaction solution resulted in much-diminished coupling rates. Likewise, the *N*-methyl imide **5b** showed slower coupling. These diminutions are hard to rationalize as steric effects at a site so remote from the reaction center. Our early excitement quickly

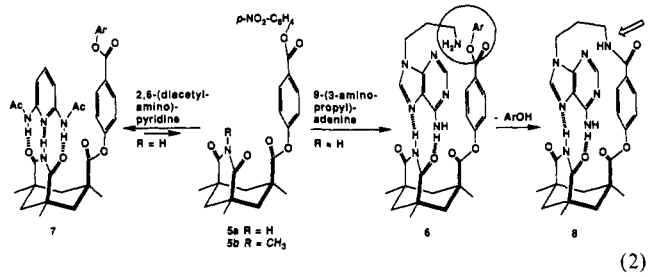

(2)

faded when the structure of the product was examined by NMR. Spectra of **8** obtained at various dilutions showed no downfield shift of the imide resonance, an indication of intramolecular base-pairing. Moreover, addition of other adenine derivatives did not affect this resonance, and all attempts to pry it open failed to affect the imide N–H resonance at about 12.4 ppm in $CDCl_3$. Further, NOE experiments indicated that the molecule remained folded shut in a Hoogsteen sense; irradiation of the imide NH enhanced H_8 of the adenine but did not enhance H_2. The molecule remained closed in the smug, self-satisfied sense of a rusted jackknife, impervious to external lubricants.

It is too painful to recount in detail the experiments with the second generation system. Suffice to say, it also raised the gloomy prospects of early extinction. The problem was that the product molecules remained stuck together in a *bimolecular* fashion as the dimer (eq 3). However, these problems suggested that building a "bulge" in the middle of the structure could help pry the dimer apart and then lead to the desired templation. Accordingly, we explored the possibility of using a ribosyl derivative as the adenine component.

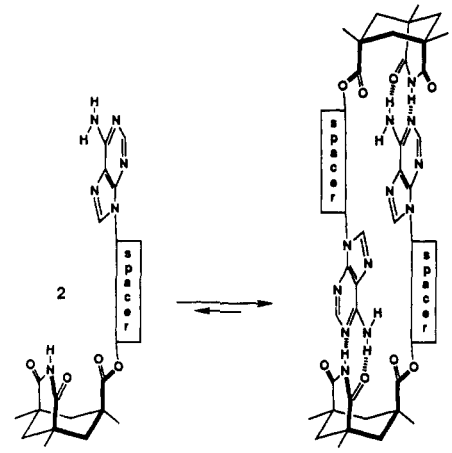

(3)

We had already observed the diminution of affinity of the ribosyl (vs ethyl) derivatives of adenine toward these imides.[12]

(7) Rebek, J., Jr. *Acc. Chem. Res.* **1984**, *17*, 258–264.
(8) For example, see: Shinkai, S.; Nakaji, T.; Ogawa, T.; Shigematsu, K.; Manabe, O. *J. Am. Chem. Soc.* **1981**, *103*, 111–115.
(9) For recent reviews, see: (a) Schultz, P. G. *Science* **1988**, *240*, 426–433. (b) Huse, W. D.; Sastry, L.; Iverson, S. A.; Kang, A. S.; Alting-Mees, M.; Burton, D.; Benkovic, S. J.; Lerner, R. A. *Science* **1989**, *246*, 1275–1281.
(10) Wolfenden, R. *Acc. Chem. Res.* **1972**, *5*, 10–18.
(11) Kemp, D. S.; Petrakis, K. S. *J. Org. Chem.* **1981**, *46*, 5140–5143.
(12) (a) Askew, B.; Ballester, P.; Buhr, C.; Jeong, K. S.; Jones, S.; Parris, K.; Williams, K.; Rebek, J., Jr. *J. Am. Chem. Soc.* **1989**, *111*, 1082–1090. (b) Williams, K.; Askew, B.; Ballester, P.; Buhr, C.; Jeong, K. S.; Jones, S.; Rebek, J., Jr. *J. Am. Chem. Soc.* **1989**, *111*, 1090–1094.
(13) Rebek, J., Jr.; Askew, B.; Ballester, P.; Buhr, C.; Costero, A.; Jones, S.; Williams, K. *J. Am. Chem. Soc.* **1987**, *109*, 6866–6867.
(14) Leonard, N. J.; Lambert, R. F. *J. Org. Chem.* **1969**, *34*, 3240–3248.

The fully blocked sugar provided some steric bulk adjacent to the aromatic-stacking surface. It seemed likely, therefore, that two such spherical lumps, near one another and with no particular affinity for each other, would destabilize the dimer. Accordingly, the 5′-aminoadenosine derivative **9** was prepared by standard procedures,[15] and its coupling reactions to imides bearing 2,6-naphthalene surfaces (**10**) were examined (eq 4). The reaction

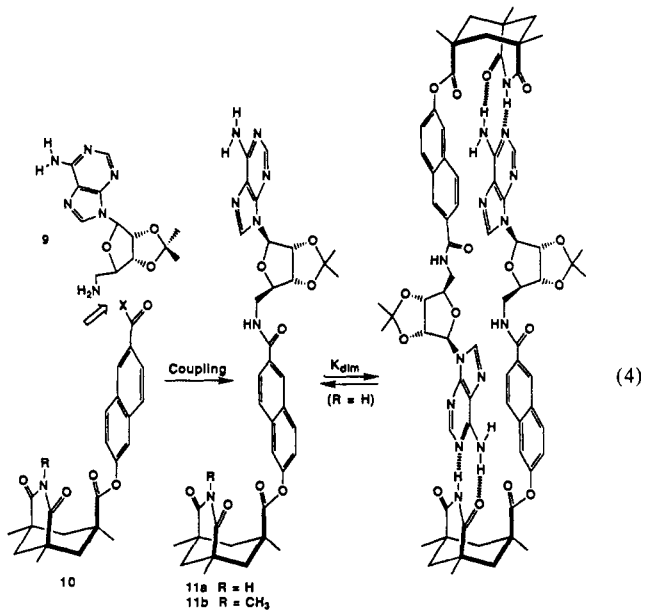

(4)

with the acid chloride was too fast to follow conveniently, whereas that of the nitrophenyl ester was too slow. The amide adduct **11a** *was* formed, and its self-affinity was suitable. Dilution studies gave a value for K_{dim} of 630 M^{-1} for the product; the bulge was doing its job. Moreover, preliminary experiments with additives such as 9-ethyladenine *slowed* the coupling rate, *but adding the reaction product speeded it up*! The active ester selected for the detailed studies was the pentafluorophenyl derivative.

The preparation of compounds used in these studies was straightforward. The syntheses of the imide derivatives **10a–d** and the *N*-methyl analogues **10e–h** are outlined in eq 5. Kemp's triacid **1** was converted to the imide acid chloride **2b** as previously described.[12] Coupling of **2b** to the naphthol **12c** generated ester **10a**. Deprotection (H_3O^+, acetone), conversion to the acid chloride ($SOCl_2$), and reaction with pentafluorophenol and triethylamine gave the pentafluorophenyl ester **10d**. The *N*-methyl derivatives **10e–h** were prepared in a similar fashion.

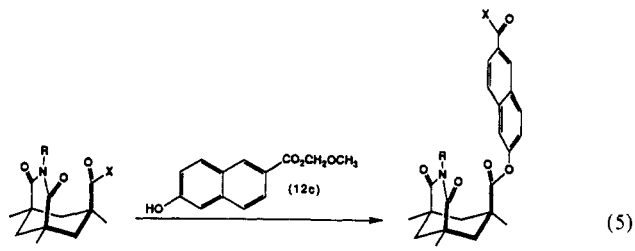

(5)

Results

Association Constants of the Components. The association constants of the various components toward one another were determined by means of NMR titrations.[12] The experimental data for associations are shown in Scheme II. From these data, a value of $K_a \approx 60$ M^{-1} for the association of imides **10d** or **11a** with adenosyl derivatives appears most relevant to the discussion that

Scheme II

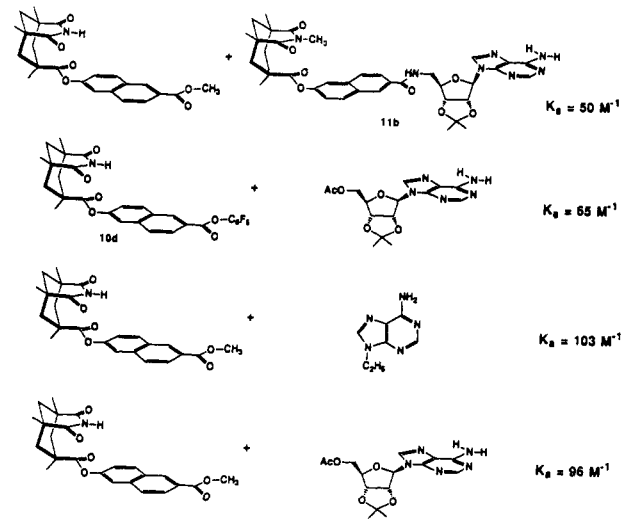

follows. In conjunction with the dimerization constant K_{dim} of template **11a**, this value can quantitate the effect that the bulge in the middle of the molecule has on its dimerization. If the two ends show identical affinity, then the K_{dim} expected would be at least $(K_a)^2$. It should actually be more because loss of translational entropy would not be required twice, as is the case in the chelate effect.[16] Bulges exist in both the Watson–Crick and Hoogsteen senses, and NOE experiments showed no particular bias in the arrangement of the dimer. Modeling suggests that the stacking is better when base-pairing occurs in the Watson–Crick form. We assume that the modest value of K_{dim} (630 M^{-1}) reflects that the ribose acetonides in the middle of the dimer interact sterically.

Kinetics Studies. Having established that template **11a** catalyzes the coupling of amine **9** and ester **10d**, we set out to quantitatively determine the rate of reaction. Continuous assay by NMR was desirable, but concentration-dependent shifts, broad NH resonances, and overlapping multiplets did not permit the accuracy (by integration) necessary to determine the relative concentration of each component. Instead, HPLC was used as the analytical method. In typical kinetic experiments, a solution of the reactants and template in $CHCl_3$ was analyzed periodically. Triethylamine was added to complex the liberated phenol and to help prevent its protonation of the aminoadenosine during the course of the reaction. All of the coupling reactions were performed with an excess of this material present (generally 4 equiv). Identical rates were observed in the presence of 4 and 8 equiv of triethylamine.

Reactions of amine **9** and pentafluorophenyl ester **10d** were studied at 1.65, 8.2, and 16.5 mM concentrations. In experiments in which template **11a** was added, 0.2 or 0.5 equiv was employed. The template and amine proved to be the best species to monitor. Competing processes, such as hydrolysis of the pentafluorophenyl ester moiety by adventitious water (especially under dilute conditions or in longer runs), limit somewhat the accuracy of the data. Nevertheless, the reproducibility of the kinetic behavior and the coupling rates was very good.

Preliminary studies were performed at 8.2 mM concentration of reactants **9** and **10d** (Figure 1). The effect of added template and inhibitor upon the rates of reaction was examined. The initial rates of reaction were calculated by linear least-squares analysis of data collected during the first 60 min of the reaction. An initial rate of 1.00×10^{-5} M min^{-1} was observed for the reaction of **9** and **10d** (Figure 1a). In the presence of added template **11a**, a significant rate increase occurs. When 0.20 equiv of **11a** is added, the initial rate increases by 43% (1.43×10^{-5} M min^{-1}, Figure 1b); when 0.50 equiv is added, the rate increases by 73% (1.73×10^{-5} M min^{-1}, Figure 1c). 2,6-bis(acetylamino)pyridine inhibits the reaction; addition of 1 equiv reduces the rate to 0.49×10^{-5}

(15) Kolb, M.; Danzin, C.; Barth, J.; Claverie, N. *J. Med. Chem.* **1982**, *25*, 550–556.

(16) For recent, dramatic examples in cyclodextrin chemisry, see: Breslow, R.; Chung, S. *J. Am. Chem. Soc.* **1990**, *112*, 9659–9660.

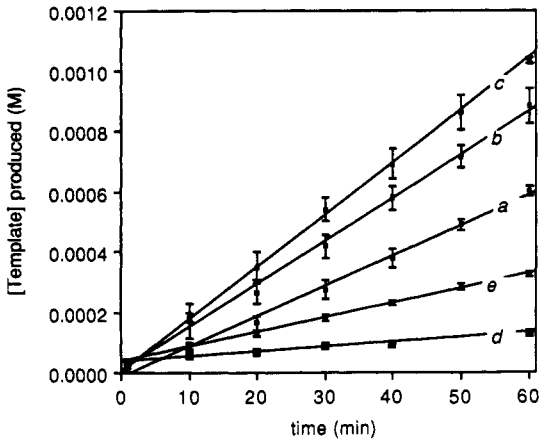

Figure 1. Generation of template **11a** or **11b** as a function of time. All reactions were performed with initial concentrations [**9**] = [**10d** or **10h**] = 0.0082 M in $CHCl_3$. Lines are linear least-squares fit of data and correspond to the initial rates of reaction. Error bars represent standard deviations of multiple independent runs. (a) Reaction of **9** and **10d**. (b) Reaction of **9** and **10d** with 0.20 equiv of **11a** added as autocatalyst. (c) Reaction of **9** and **10d** with 0.50 equiv of **11a** added as autocatalyst. (d) Reaction of **9** and the N-methylated **10h** (single run). (e) Reaction of **9** and **10d** with 1 equiv of 2,6-bis(acetylamino)pyridine added as inhibitor.

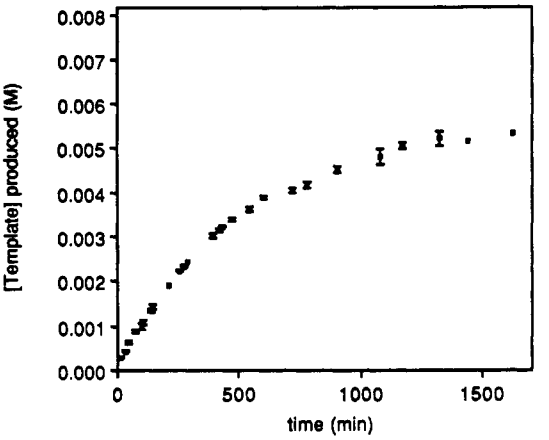

Figure 2. Generation of template **11a** as a function of time. The initial concentrations: [**9**] = [**10d**] = 0.0082 M in $CHCl_3$. Error bars represent standard deviations of multiple independent runs.

Table I. Initial Rates of Reaction of Amine **9** and Ester **10d** or **10h**

reactants	additive	rate (M min^{-1})[a]
8.2 mM **9**, **10d**	none	$(1.00 \pm 0.06) \times 10^{-5}$
8.2 mM **9**, **10d**	0.20 equiv of **11a**	$(1.43 \pm 0.05) \times 10^{-5}$
8.2 mM **9**, **10d**	0.50 equiv of **11a**	$(1.73 \pm 0.12) \times 10^{-5}$
8.2 mM **9**, **10d**	1.00 equiv of 2,6-bis-(acetylamino)pyridine	$(0.49 \pm 0.03) \times 10^{-5}$
8.2 mM **9**, **10h**	none	0.15×10^{-5} [b]
16.5 mM **9**, **10d**	none	$(5.6 \pm 0.2) \times 10^{-5}$
16.5 mM **9**, **10d**	0.20 equiv of **11a**	$(7.4 \pm 0.4) \times 10^{-5}$
16.5 mM **9**, **10d**	0.55 equiv of **11a**	$(8.8 \pm 0.5) \times 10^{-5}$
1.65 mM **9**, **10d**	none	$(0.050 \pm 0.007) \times 10^{-5}$
1.65 mM **9**, **10d**	0.20 equiv of **11a**	$(0.065 \pm 0.007) \times 10^{-5}$

[a] Uncertainties in rates represent standard deviations of multiple (2–4) independent runs. [b] Data from a single run.

M min^{-1} (Figure 1e). The rate of the reaction of *N*-methyl imide **10h** with aminoadenosine **9** is substantially slower than that of the parent (NH) imide **10d** (0.15×10^{-5} M min^{-1}, Figure 1d). Whereas the generation of product is essentially linear during the first 60 min of reaction at 8.2 mM, the rate slows as the reaction progresses. Figure 2 illustrates the formation of product over the course of the reaction of **9** and **10d** at 8.2 mM. The apparent failure of the reaction to approach completion (8.2 mM) may arise from the hydrolysis of the pentafluoro ester group of **10d**.

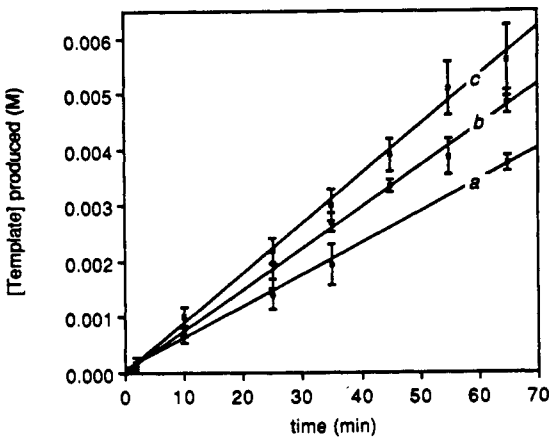

Figure 3. Generation of template **11a** as a function of time. All reactions were performed with initial concentrations [**9**] = [**10d**] = 0.0165 M in $CHCl_3$. Lines are linear least-squares fit of data and correspond to the initial rates of reaction. Error bars represent standard deviations of multiple independent runs. (a) Reaction of **9** and **10d**. (b) Reaction of **9** and **10d** with 0.20 equiv of **11a** added as autocatalyst. (c) Reaction of **9** and **10d** with 0.55 equiv of **11a** added as autocatalyst.

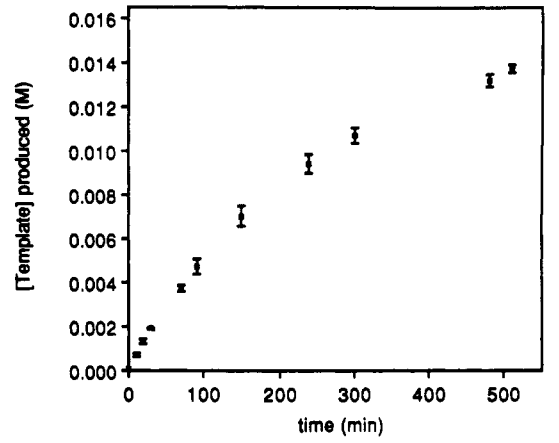

Figure 4. Generation of template **11a** as a function of time. The initial concentrations: [**9**] = [**10d**] = 0.0165 M in $CHCl_3$. Error bars represent standard deviations of multiple independent runs.

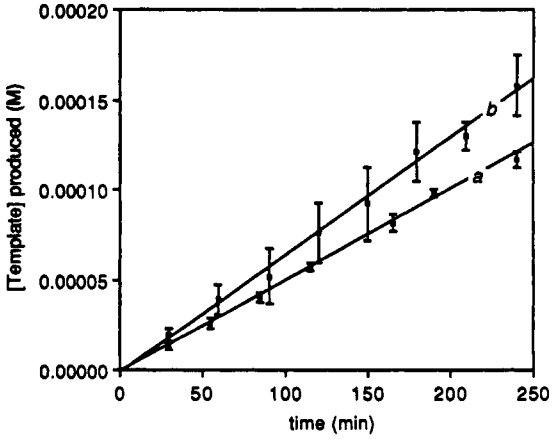

Figure 5. Generation of template **11a** as a function of time. All reactions were performed with initial concentrations [**9**] = [**10d**] = 0.001 65 M in $CHCl_3$. Lines are linear least-squares fit of data and correspond to the initial rates of reaction. Error bars represent standard deviations of multiple independent runs. (a) Reaction of **9** and **10d**. (b) Reaction of **9** and **10d** with 0.20 equiv of **11a** added as autocatalyst.

The reaction of **9** and **10d** is considerably more rapid at 16.5 mM. The initial rates of reaction were measured during the first 65 min of the reaction (Figure 3). Rates of 5.6×10^{-5}, 7.4×10^{-5}, and 8.8×10^{-5} M min^{-1} were observed for reaction in the

presence of 0, 0.20, and 0.55 equiv of added template **11a**, respectively. Figure 4 illustrates the prolonged course of the reaction of **9** and **10d**.

At 1.65 mM, the reaction of **9** and **10d** is far slower. Initial rates of 0.050×10^{-5} and 0.065×10^{-5} M min^{-1} occurred in the presence of 0 and 0.20 equiv of added template **11a** (Figure 5). Table I summarizes the rate data described in this section.

Discussion

Three reactions contribute to the formation of product: the *background bimolecular* reaction, the *base-paired bimolecular* reaction, and the *termolecular template-catalyzed* process. The latter reaction is responsible for the replication process. Their interplay determines the shape of the kinetic curves.

Background Bimolecular Reaction. The aminoadenosine **9** reacts with the pentafluorophenyl ester **10d** by means of a bimolecular reaction, as shown in eq 6. The background bimolecular reaction was established with the *N*-methyl imide derivative of the pentafluorophenyl ester **10h** as the acylating agent. The rate

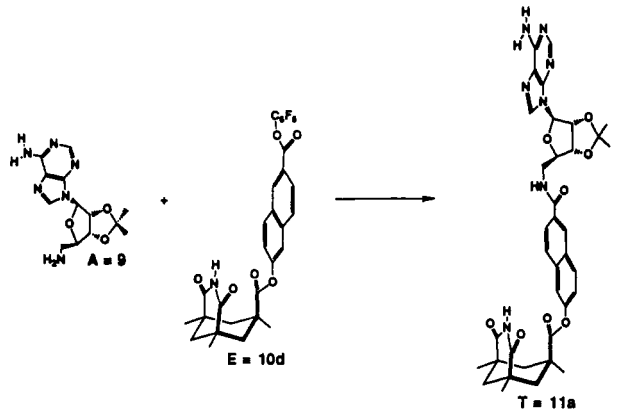

(6)

constant for this process is 0.023 M^{-1} min^{-1}. An independent measure of the background bimolecular rate, using 2,6-bis(acetylamino)pyridine as an inhibitor (K_a = 450 M^{-1}) in the reaction of **9** with the parent (NH) derivative **10d**, gave a value consistent with that obtained from the *N*-methyl compound **10h** (vide infra).

Base-Pairing or Preassociative Mechanism. A second pathway, in which amine **9** and ester **10d** form a hydrogen-bonded dimer AE prior to reaction, has a far greater role in the generation of template **11a** (eq 7). In this complex, the amino and pentafluorophenyl groups are in close proximity and readily react to generate the template in its cis amide conformation, *cis*-T. Isomerization to the more stable trans amide occurs rapidly.

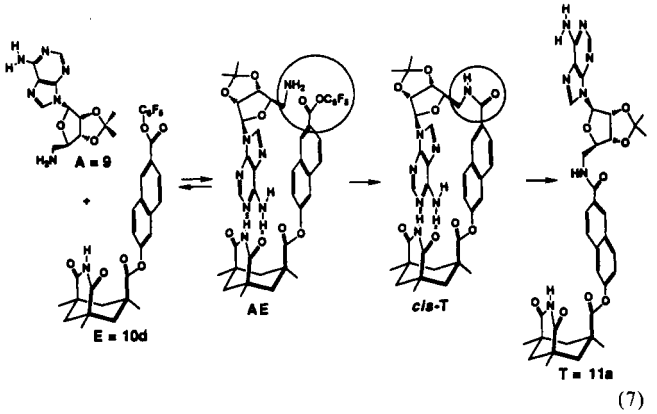

(7)

That the NH derivative **10d** reacts 6.5-fold more rapidly with the aminoadenosine **9** than the *N*-methyl derivative **10h** under the same conditions provides strong evidence for this preassociative mechanism (Table I). The inhibition of the reaction of **9** and **10d** by 2,6-bis(acetylamino)pyridine provides additional evidence. A decrease in the rate of reaction corresponding to the decrease in the fraction of base-paired complex is observed. From the base-pairing association constant between **9** and **10d** (ca. 60 M^{-1}; vide supra), it can be calculated that the initial mixture at 8.2×10^{-3} M concentration involves 27% base-paired and 73% free components. The former contribute to the preassociative mechanism, whereas the latter contribute to the background reaction. When 1 equiv of 2,6-bis(acetylamino)pyridine (K_a = 450 M^{-1} with **10d**) is added to this mixture, the fraction of free ester **10d** decreases to 32%. While the ester that is complexed with 2,6-bis(acetylamino)pyridine (54%) should still be reactive toward amine **9** via the background bimolecular pathway, it is unable to participate in the preassociative mechanism. The fraction of base pair is calculated to be 14% (51% of the value in the absence of the inhibitor), while the observed rate is 48% of the value in the absence of inhibitor (Table I).

Termolecular Template Process. The template-catalyzed, replicative process (eq 8) was revealed by the enhanced rate of reaction of amine **9** and ester **10d** upon addition of the template product **11a** to coupling mixtures. In this mechanism, the amine,

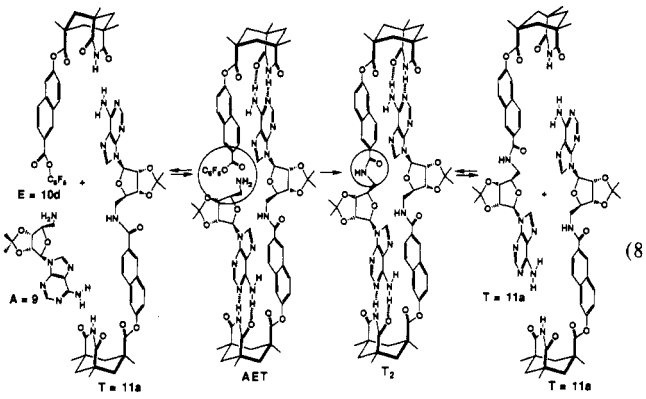

(8)

ester, and template first form a termolecular complex, AET. The close proximity of the reactive amino and pentafluorophenyl ester groups then leads to amide formation. The resulting template dimer T_2 exists in equilibrium with the free template.[17] Control experiments with the *N*-methyl imide product **11b** showed that its presence did not increase (or significantly decrease) the rate of product formation.

Kinetic Modeling of the Replication Process. The self-replicating system contains a variety of species in rapid equilibrium. For the purposes of this discussion, we have assigned easily identified letter names (shown in eqs 6–8) to these species. At millimolar concentrations, there are substantial amounts of the bimolecular species AE, AT, ET, and T_2 and some termolecular complex AET in addition to the free amine A (**9**), ester E (**10d**), and template T (**11a**). Equations 9–14 represent all significant complexation processes. The values of the various equilibrium constants were determined by extrapolation from the related systems shown in Scheme II, from which K_1, K_2, and K_3 were each estimated to be 60 M^{-1}. The absence of steric or electronic communication between the two ends of the template suggests that K_4 and K_5 should have the similar values. The value of the self-association constant of the template, K_{dim}, is 630 M^{-1} (vide supra).

$$A + E \overset{K_1}{\rightleftharpoons} AE \quad (9)$$

$$A + T \overset{K_2}{\rightleftharpoons} AT \quad (10)$$

$$E + T \overset{K_3}{\rightleftharpoons} ET \quad (11)$$

$$A + ET \overset{K_4}{\rightleftharpoons} AET \quad (12)$$

$$E + AT \overset{K_5}{\rightleftharpoons} AET \quad (13)$$

$$2T \overset{K_{dim}}{\rightleftharpoons} T_2 \quad (14)$$

(17) For an excellent analysis of related termolecular processes, see: Kelly, T. R.; Bridger, G. J.; Zhao, C. *J. Am. Chem. Soc.* **1990**, *112*, 8024–8034.

Table II. Concentrations (M) of Species Present[a]

$[C]_{tot}$	[A] = [E]	[T]	[AE]	[AT] = [ET]	[AET]	$[T_2]$
0	0.007 03	0	0.002 97	0	0	0
0.001	0.006 91	0.000 40	0.002 86	0.000 17	0.000 07	0.000 10
0.003	0.006 74	0.000 95	0.002 72	0.000 38	0.000 15	0.000 57
0.010	0.006 39	0.002 16	0.002 46	0.000 83	0.000 32	0.002 93

[a] $[A]_{tot} = [E]_{tot} = 0.010$ M.

The three pathways by which template is generated were described above. (1) In the background bimolecular pathway, the amine A and ester E react without preassociation to give the template T, with a rate constant of k_1 (eq 15). Hydrogen-bonded species (i.e., AE, AT, ET, and AET) can also react with each other by means of this bimolecular pathway. (2) In the base-paired bimolecular pathway, the hydrogen-bonded complex AE reacts to generate the template, initially in an unstable cis amide conformation with a rate constant of k_2 (eq 16). Isomerization to the more stable trans conformation is assumed to be a rapid, thermodynamically favorable process. (3) In the autocatalytic, template termolecular pathway the template forms via the complex AET with a rate constant of k_3 (eq 17).

$$A + E \xrightarrow{k_1} T \quad (15)$$

$$AE \xrightarrow{k_2} T \quad (16)$$

$$AET \xrightarrow{k_3} T_2 \quad (17)$$

Kinetic modeling of the overall process was performed with use of an iterative numerical method.[18] Fitting of the observed data from experiments performed at 8.2×10^{-3} M in amine **9** and ester **10d** or **10h** generates values of 0.023 M^{-1} min^{-1}, 0.0036 min^{-1}, and 0.070 min^{-1} for k_1, k_2, and k_3, respectively. Rate constants were determined by minimizing the least-squares difference between observed and calculated values and also by matching of the calculated and experimental initial rates of reaction. Figure 6 shows the calculated vs experimental formation of template as a function of time. A satisfactory fit was obtained within the limits of the precision of the data.[19] (The discrepancy between curve d and the corresponding data points arises from the presence of a small quantity of N-methylated template **11b** at the beginning of the experiment.)

A number of systematic errors limit the accuracy of these rate constants. Notable are variations in temperature, evaporative losses of solvent during prolonged runs, and slow hydrolysis of the ester by adventitious H_2O. The rate constants were found to fit other reaction conditions only moderately well. The initially observed rate of reaction of **9** and **10d** at 1.65 mM was calculated to be 18 times slower than that at 8.2 mM, whereas a 20-fold slower rate was actually observed (Table I). The initially observed rate of reaction of **9** and **10d** at 16.5 mM was calculated to be 3.3 times as fast as that at 8.2 mM, while a 5.6-fold greater rate was observed (Table I). A portion of this discrepancy appears to arise from systematic errors, however. When the same stock solutions of **9** and **10d** were used for both the 16 and the 8 mM runs, only a 4.2-fold greater rate was observed. In all cases, the kinetic model predicted the observed trends in reactivity quite well. That some quantitative variations from the model are observed may indicate the limitations of the model, as well as systematic experimental errors.

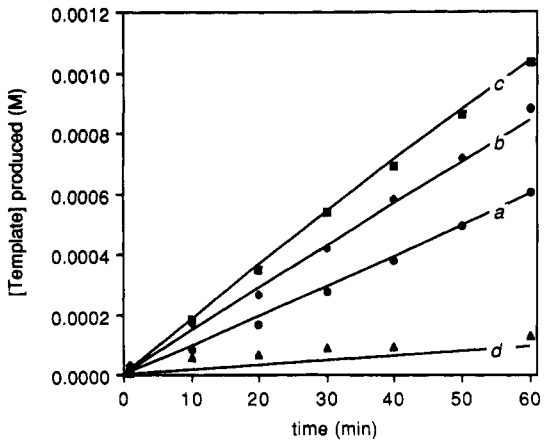

Figure 6. Experimental (points) and calculated (lines) generation of template **11a** or **11b** as a function of time. All reactions were performed with initial concentrations [**9**] = [**10d** or **10h**] = 0.0082 M in $CHCl_3$. (a) Reaction of **9** and **10d**. (b) Reaction of **9** and **10d** with 0.20 equiv of **11a** added as autocatalyst. (c) Reaction of **9** and **10d** with 0.50 equiv of **11a** added as autocatalyst. (d) Reaction of **9** and the N-methylated **10h**.

The ratio of the rate constants of an intramolecular reaction and its intermolecular counterpart corresponds to the "effective molarity" of the reacting groups in the intramolecular reaction and thereby provides an index of the efficiency of the intramolecular process. Reaction by means of the hydrogen-bonded complexes (AE and AET in eqs 16 and 17) constitutes intramolecular processes that can be compared to the bimolecular reaction (eq 15). It is interesting to note that the effective molarities of the amine and ester groups are actually *higher* in the termolecular complex AET than in the bimolecular complex AE (k_3/k_1 = 3.0 M, k_2/k_1 = 0.16 M). This 19-fold difference in effective molarity may reflect a higher activation energy for formation of the cis conformation of amide **11a** from the bimolecular complex AE or a more favorable arrangement of functional groups in the termolecular complex AET. It is generally difficult to compare reactions of different orders because of differing trajectories and stereoelectronic effects.[20]

In spite of the greater effective molarity in the termolecular complex, a large fraction of the product forms by the preassociative bimolecular pathway because of the difference in molecularity of the two processes. Under typical reaction conditions (e.g., 10^{-2} M concentration of reactants), the concentration of the bimolecular complex far exceeds the concentration of the termolecular complex. Table II illustrates the concentrations of individual species (A, E, T, AE, AT, ET, AET, T_2) present as a function of the total concentrations of species containing amine, ester and template ($[A]_{tot}$, $[E]_{tot}$, $[T]_{tot}$: $[A]_{tot} = [A] + [AE] + [AT] + [AET]$; $[E]_{tot}$

(18) The course of the reaction was treated as 100 time increments, Δt. Equilibrium concentrations of A, E, T, AE, AT, ET, T_2, and AET were calculated at each time increment by using successive approximations. The incremental formation of template was calculated by the equation: $\Delta[T]_{tot} = k_1[A]_{tot}[E]_{tot}\Delta t + k_2[AE]\Delta t + k_3[AET]\Delta t$, in which $[A]_{tot}$, $[E]_{tot}$, and $[T]_{tot}$ represent the total concentrations of amine, ester, and template present. Calculations were performed on a Macintosh computer with Microsoft Excel.

(19) An alternative model for the kinetics of self-replicating systems was introduced by von Kiedrowski in 1986. (See refs 5a–c.) In this model, the rate is given as the sum of an autocatalytic term and a background term. The magnitude of the autocatalytic term is proportional to the square root of the total concentration of template, i.e., rate = $k_a[A]_{tot}[E]_{tot}[T]_{tot}^{1/2} + k_b[A]_{tot}[E]_{tot}$. While this model is primarily applicable to systems in which the template predominantly exists as the dimer, such as oligonuclotides, it fits the data presented in the results section quite well. We found the best fit rate constants to be $k_a = 4 \times 10^{-2}$ $M^{-3/2}$ s^{-1} and $k_b = 2 \times 10^{-3}$ M^{-1} s^{-1}. These values differ substantially from the values $k_a = 9.87 \times 10^{-2}$ $M^{-3/2}$ s^{-1} and $k_b = 1.24 \times 10^{-3}$ M^{-1} s^{-1}, which von Kiedrowski reports for our system (ref 5c). The von Kiedrowski model provides a simple, elegant, and effective means of obtaining the kinetic parameters of autocatalytic systems without the need for equilibrium constants. The model presented in this paper accounts for the mechanistic details of the reaction and for the role of each of the three mechanistic pathways (background bimolecular, preassociative, and template termolecular). This model permits specific predictions about the effects of changes in structure and binding affinities upon the rates of reaction.

(20) For a discussion with leading references, see: Kemp, D. S.; Galakatos, N. G.; Bowen, B.; Tan, K. *J. Org. Chem.* **1986**, *51*, 1829–1838.

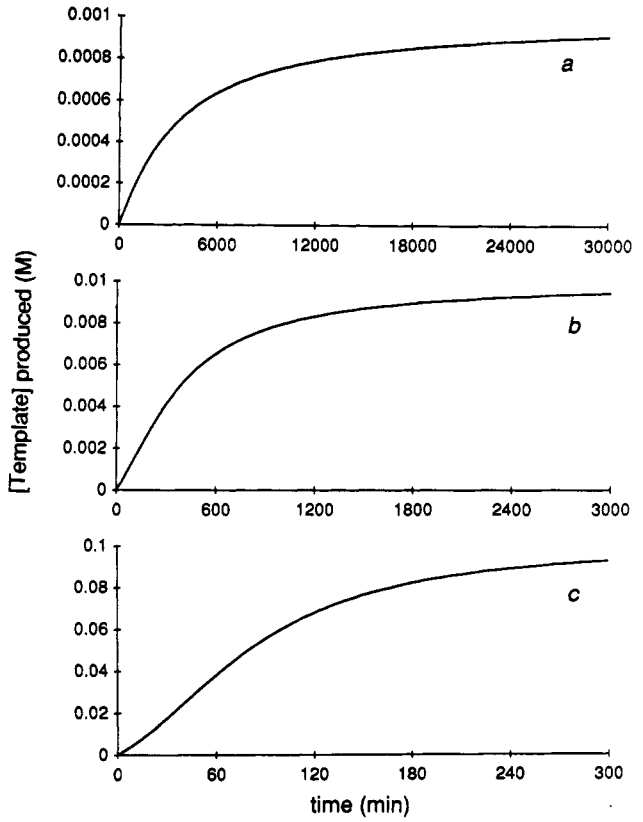

Figure 7. Calculated effect of reactant concentration upon the growth curve. All calculations were performed with the experimentally determined rate and equilibrium constants (see text). (a) Top, initial concentrations: [**9**] = [**10d**] = 0.001 M. (b) Middle, initial concentrations: [**9**] = [**10d**] = 0.01 M. (c) Bottom, initial concentrations: [**9**] = [**10d**] = 0.1 M.

= [E] + [AE] + [ET] + [AET]; $[T]_{tot}$ = [AT] + [ET] + [AET] + 2[T_2]). For example, in the presence of 0.3 equiv of added template ($[A]_{tot}$ = $[E]_{tot}$ = 0.010 M, $[T]_{tot}$ = 0.003 M), 67% of the amine and ester are free, 27% are associated with each other, and 1.5% are present as the termolecular complex. Under these conditions, the relative rates of the background bimolecular pathway, the preassociative pathway, and the template termolecular pathway are 1.0:4.3:4.6, respectively. While the background bimolecular reaction contributes only slightly to the formation of product, both the preassociative (uncatalyzed) and the template (autocatalytic) mechanisms contribute substantially.

Of particular interest is the shape of the product growth curve. In a system in which *most of the product* forms by an autocatalytic pathway, a sigmoidal growth curve is expected.[21] Even so, sigmoidal growth has been difficult to observe in a self-replicating system.[3,5,23] Our model predicts that the initial concentration of reactants should substantially affect the shape of the growth curve. At concentrations on the order of 10^{-3} M, the contribution of the autocatalytic pathway is insignificant in our system, and the reaction profile is similar to that of the simple bimolecular kinetics (Figure 7a). A slight sigmoidal shape should be observed at initial concentrations in the order of 10^{-2} M (Figure 7b). Unfortunately, the degree of sigmoidal curvature is small in comparison to the uncertainty in the data points and is not observable. At concentrations on the order of 10^{-1} M, a significantly sigmoidal growth curve is anticipated (Figure 7c). Limitations

(21) The occurrence of sigmoidal growth can be established graphically by examining plots of the first or second derivative of [product] vs time (t). The magnitude of the sigmoidal growth can be quantified as the ratio of the *maximal* value of d[T]/dt (or Δ[T]/Δt) to the *initial* value of d[T]/dt (or Δ[T]/Δt).

(22) For a self-replicating system of reverse micelles, see: Bachmann, P. A.; Walde, P.; Luisi, P. L.; Lang, J. *J. Am. Chem. Soc.* **1990**, *112*, 8200–8201.

(23) For a recently published exception, see ref 5c.

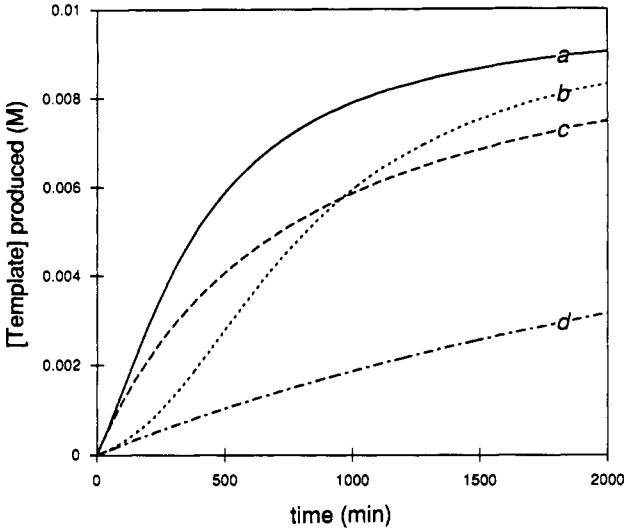

Figure 8. Calculated effect of rate constants k_1, k_2, and k_3 upon the growth curve. All calculations were performed for initial concentrations [**9**] = [**10d**] = 0.01 M with the experimentally determined equilibrium constants (see text). (a) k_1 = 0.023 M^{-1} min^{-1}, k_2 = 0.0036 min^{-1}, k_3 = 0.070 min^{-1}. (b) k_1 = 0.023 M^{-1} min^{-1}, k_2 = 0, k_3 = 0.070 min^{-1}. (c) k_1 = 0.023 M^{-1} min^{-1}, k_2 = 0.0036 min^{-1}, k_3 = 0. (d) k_1 = 0.023 M^{-1} min^{-1}, k_2 = 0, k_3 = 0.

of solubility prevented our studying the reaction at concentrations in which substantial sigmoidal behavior is expected.

We have also used this model to predict the effects of changes in the rate constants upon the shape of the growth curve (Figure 8). Curve a represents the reaction profile calculated for typical reaction conditions (0.010 M initial concentration of **9** and **10d**) with the experimentally determined rate constants (k_1 = 0.023 M^{-1} min^{-1}, k_2 = 0.0036 min^{-1}, and k_3 = 0.070 min^{-1}). A slight inflection is calculated in this curve, but it is too small to be observed experimentally (vide supra). If the preassociative bimolecular pathway were not operative (i.e., k_1 = 0.023 M^{-1} min^{-1}, k_2 = 0, and k_3 = 0.070 min^{-1}), then a highly sigmoidal growth curve b would be observed. For comparison, curve c represents the growth curve in the absence of an autocatalytic mechanism (i.e., k_1 = 0.023 M^{-1} min^{-1}, k_2 = 0.0036 min^{-1}, and k_3 = 0), and curve d corresponds to reaction by a simple bimolecular mechanism (i.e., k_1 = 0.023 M^{-1} min^{-1}, k_2 = 0, and k_3 = 0). Needless to say, both c and d lack inflection points. Structurally modified molecules in which the electrophile and nucleophile are at a sufficient distance in the base-paired, bimolecular complex such that the preassociative bimolecular pathway is not possible (i.e., k_2 = 0) are now in hand. We will report upon these studies in due course.

Conclusion and Outlook

In this paper we have provided a detailed description of the design, synthesis, and study of a molecular template, **11a**, that catalyzes its own formation from simpler components, **9** and **10d**. Together, the components and template make up a self-replicating system. Three reaction pathways lead to the formation of template, yet only one, the template termolecular process, is responsible for replication. A kinetic model for the replication process has been developed. Modeling studies indicate that both the preassociative mechanism and the template termolecular process contribute substantially to the formation of template. Calculations predict that a system in which the preassociative mechanism cannot operate will self-replicate efficiently and will exhibit a highly sigmoidal growth curve.

The fundamental feature of our self-replicating system is self-complementarity. It may now be easier to visualize other possibilities.[22] The fixation on double-stranded nucleic acids is natural, and their catalytic features suggest their originality. What other structures can be considered? We mention two beyond the current system. The first involves hybrid structures of amino acids with nucleic acids. For the second, we have identified naturally occurring peptides that show the requisite structural features.

Whether these live up to their promise in catalyzing their own replication is the subject of our current efforts.

Experimental Section

General. Mass spectra were obtained on a VG Instrument, an Se-20 mass spectrometer, or a Varian CH-5 instrument (high resolution). IR spectra were obtained on an IBM IR/32 FTIR. ^{1}H NMR spectra were obtained on 250- and 300-MHz Bruker instruments. THF was distilled from sodium benzophenone ketyl. CH_2Cl_2 was distilled from CaH_2.

***N*-Methyl Imide Acid 2c.** To 1.0 g of Kemp's triacid anhydride[12] (1.55 mmol) was added 15 mL of a 40% aqueous solution of methylamine, and the resulting solution was heated (60 °C) overnight. The solution was allowed to cool, and excess methylamine was evaporated under reduced pressure. The solution was acidified with concentrated HCl to pH 1 and cooled to 0 °C. The resulting suspension was filtered, washed with water, and dried at 110 °C under vacuum for 3 h to afford 0.90 g (80%) of **2c** as a white solid: mp 263–265 °C; ^{1}H NMR (300 MHz, $CDCl_3$) δ 11.0 (s, 1 H), 2.71 (s, 3 H), 2.55 (d, J = 13.6 Hz, 2 H), 1.99 (d, J = 13.3 Hz, 1 H), 1.37 (d, J = 13.3 Hz, 1 H), 1.27 (s, 6 H), 1.21 (s, 3 H), 1.21 (d, J = 13.5 Hz, 2 H).

***N*-Methyl Imide Acid Chloride 2d.** Reaction of N-methyl imide acid **2c** (5.0 g, 18.4 mmol) with $SOCl_2$ (100 mL) was performed as described for the preparation of **2b**[12] to afford 5.0 g (97%) of **2d** as a pale yellow solid. An analytical sample was prepared by recrystallization from EtOAc as colorless crystals: mp 120–122 °C; IR (KBr) 3200, 3094, 2987, 1780, 1721, 1696, 1462, 1385, 1205, 924, 897, 833 cm^{-1}; ^{1}H NMR (300 MHz, $CDCl_3$) δ 2.90 (s, 3 H), 2.78 (d, J = 14.6 Hz, 2 H), 2.04 (d, J = 13.4 Hz, 1 H), 1.43 (d, J = 14.5 Hz, 2 H), 1.37 (s, 3 H), 1.32 (s, 6 H), 1.27 (d, J = 13.3 Hz, 1 H).

Imide Ester 10a. A 200-mL, round-bottom flask was charged with imide acid chloride **2b**[12] (0.38 g, 1.47 mmol), **12c** (0.34 g, 1.47 mmol), and dry methylene chloride (ca. 50 mL). 4-(Dimethylamino)pyridine (ca. 10 mg) and 2 mL of triethylamine were added and the resulting solution was stirred under nitrogen for 12 h. The solution was washed with 1 N HCl (ca. 20 mL), water (2 × 20 mL), and brine (20 mL), dried over $MgSO_4$, filtered, and evaporated to give a yellow solid. Column chromatography on silica gel (5% EtOAc in $CHCl_3$) afforded 0.54 g (81%) of **10a** as a white solid: mp 185–187 °C: ^{1}H NMR (300 MHz, $CDCl_3$) δ 8.64 (s, 1 H), 8.10 (dd, J = 1.4, 8.8 Hz, 1 H), 7.95 (d, J = 8.9 Hz, 1 H), 7.86 (d, J = 8.6 Hz, 1 H), 7.61 (s, 1 H), 7.59 (s, 1 H), 7.26 (m, 1 H), 5.55 (s, 2 H), 3.60 (s, 3 H), 2.88 (d, J = 14.2 Hz, 2 H), 2.08 (d, J = 13.2 Hz, 1 H), 1.49 (s, 3 H), 1.44 (d, J = 13.2 Hz, 1 H), 1.35 (d, J = 14.2 Hz, 2 H), 1.34 (s, 6 H); HRMS m/z (M^+) calcd 453.1787, obsd 453.1753.

Imide Acid 10b. A solution of imide ester **10a** (0.41 g, 0.90 mmol) in acetone (ca. 20 mL) and 5 drops of concentrated HCl was heated at 50 °C for 2 h. The solvent was evaporated, and a solid was obtained. The solid was dissolved in 50 mL of EtOAc, and the solution was washed with brine, dried over $MgSO_4$, filtered, and concentrated to afford 0.33 g (89%) of **10b** as a tan solid: mp 295–300 °C; ^{1}H NMR (300 MHz, $CDCl_3$) δ 10.57 (s, 1 H), 7.88 (s, 1 H), 7.63 (m, 4 H), 7.19 (dd, J = 2.1, 8.7 Hz, 1 H), 2.90 (d, J = 13.8 Hz, 2 H), 2.14 (d, J = 13.5 Hz, 1 H), 1.50 (d, J = 13.5 Hz, 1 H), 1.47 (s, 3 H), 1.37 (s, 6 H), 1.29 (d, J = 13.2 Hz, 2 H); HRMS m/z (M^+) calcd 409.1525, obsd 409.1533.

Imide Acid Chloride 10c. A suspension of imide acid **10b** (0.33 g, 0.80 mmol), $SOCl_2$ (2 mL), and 1 drop of DMF in 25 mL of dry CH_2Cl_2 was heated at 40 °C for 0.5 h. The resulting clear solution was evaporated to give 0.34 g (100%) of **10c** as a yellow solid: mp 195–200 °C; ^{1}H NMR (300 MHz, $CDCl_3$) δ 8.73 (s, 1 H), 8.07 (dd, J = 1.5, 8.7 Hz, 1 H), 8.00 (d, J = 8.9 Hz, 1 H), 7.88 (d, J = 8.7 Hz, 1 H), 7.63 (s, 1 H), 7.62 (s, 1 H), 7.31 (dd, J = 2.1, 8.8 Hz, 1 H), 2.87 (d, J = 13.5 Hz, 2 H), 2.08 (d, J = 13.3 Hz, 1 H), 1.50 (s, 3 H), 1.44 (d, J = 13.3 Hz, 1 H), 1.36 (d, J = 13.5 Hz, 2 H), 1.33 (s, 6 H); HRMS m/z (M^+) calcd 427.1186, obsd 427.1172.

Imide Ester 10d. A solution of acid chloride **10c** (0.18 g, 0.42 mmol), pentafluorophenol (0.078 g, 0.42 mmol), triethylamine (0.5 mL), and dry methylene chloride (15 mL) was heated at reflux for 12 h. The solution was allowed to cool, extracted with 10 mL of 1 N HCl and 10 mL of water, dried over $MgSO_4$, filtered, and concentrated to give a brownish residue. Column chromatography on silica gel (1:1 EtOAc–hexanes) gave 0.23 g (95%) of **10d** as a tan powder: mp 150–152 °C; ^{1}H NMR (250 MHz, $CDCl_3$) δ 8.78 (s, 1 H), 8.16 (dd, J = 1.8, 8.7 Hz, 1 H), 8.00 (d, J = 9.0 Hz, 1 H), 7.94 (d, J = 8.7 Hz, 1 H), 7.67 (s, 1 H), 7.64 (d, J = 2.2 Hz, 1 H), 7.30 (dd, J = 2.2, 8.8 Hz, 1 H), 2.88 (d, J = 13.6 Hz, 2 H), 2.09 (d, J = 13.4 Hz, 1 H), 1.50 (s, 3 H), 1.44 (d, J = 13.3 Hz, 1 H), 1.36 (d, J = 13.5 Hz, 2 H), 1.33 (s, 6 H); HRMS m/z (M^+) calcd 575.1367, obsd 575.1365.

***N*-Methyl Imide Ester 10e.** Reaction of imide acid chloride **2d** (0.65 g, 2.39 mmol) with naphthol **12c** (0.56 g, 2.39 mmol) was performed as described for the preparation of **10a** to give a yellowish oil. Column chromatography on silica gel (5% EtOAc in $CHCl_3$) afforded 0.96 g (86%) of **10e** as a white solid: mp 158–160 °C; ^{1}H NMR (300 MHz, $CDCl_3$) δ 8.63 (s, 1 H), 8.10 (dd, J = 1.5, 7.1 Hz, 1 H), 7.95 (d, J = 8.9 Hz, 1 H), 7.86 (d, J = 8.6 Hz, 1 H), 7.62 (d, J = 1.9 Hz, 1 H), 7.27 (dd, J = 2.2, 8.7 Hz, 1 H), 5.55 (s, 2 H), 3.59 (s, 3 H), 2.85 (s, 3 H), 2.84 (d, J = 7.7 Hz, 2 H), 2.03 (d, J = 7.9 Hz, 1 H), 1.46 (d, J = 7.9 Hz, 1 H), 1.45 (s, 3 H), 1.35 (d, J = 7.9 Hz, 2 H), 1.34 (s, 6 H).

***N*-Methyl Imide Acid 10f.** The ester **10e** (0.87 g, 1.86 mmol) was converted to the acid **10f** (0.65 g, 82%) as described for the preparation of **10b**: mp 255–258 °C; ^{1}H NMR (300 MHz, $CDCl_3$) δ 8.67 (s, 1 H), 8.10 (dd, J = 1.9, 8.6 Hz, 1 H), 7.96 (d, J = 9.0 Hz, 1 H), 7.88 (d, J = 8.7 Hz, 1 H), 7.63 (d, J = 1.8 Hz, 1 H), 7.30 (dd, J = 2.0, 8.9 Hz, 1 H), 2.86 (s, 3 H), 2.85 (d, J = 13.5 Hz, 2 H), 2.04 (d, J = 13.4 Hz, 1 H), 1.48 (s, 3 H), 1.47 (d, J = 13.7 Hz, 2 H), 1.35 (s, 6 H), 1.28 (d, J = 14.9 Hz, 2 H); HRMS m/z (M^+) calcd 423.1682, obsd 423.1686.

***N*-Methyl Imide Acid Chloride 10g.** The acid **10f** (0.65 g, 1.53 mmol) was converted to acid chloride **10g** (0.68 g, 100%) as described for the preparation of **10c**: mp 170–173 °C; ^{1}H NMR (300 MHz, $CDCl_3$) δ 8.73 (s, 1 H), 8.07 (dd, J = 1.9, 8.7 Hz, 1 H), 8.00 (d, J = 8.9 Hz, 1 H), 7.88 (d, J = 8.8 Hz, 1 H), 7.65 (d, J = 2.1 Hz, 1 H), 7.34 (dd, J = 2.2, 8.9 Hz, 1 H), 2.85 (d, J = 13.0 Hz, 2 H), 2.84 (s, 3 H), 2.04 (d, J = 13.2 Hz, 1 H), 1.48 (s, 3 H), 1.46 (d, J = 13.1 Hz, 1 H), 1.35 (s, 6 H), 1.34 (d, J = 14.3 Hz, 2 H); HRMS m/z (M^+) calcd 441.1343, obsd 441.1325.

***N*-Methyl Imide Ester 10h.** Acid chloride **10g** (0.18 g, 0.42 mmol) was converted to pentafluorophenol ester **10h** as described for the preparation of **10d**. Column chromatography on silica gel (1:2:2 EtOAc–hexanes–$CHCl_3$) gave 0.23 g (95%) of **10h**: mp 85–95 °C; ^{1}H NMR (250 MHz, $CDCl_3$) δ 8.79 (s, 1 H), 8.16 (dd, J = 1.8, 7.2 Hz, 1 H), 8.00 (d, J = 8.9 Hz, 1 H), 7.93 (d, J = 8.7 Hz, 1 H), 7.68 (d, J = 1.8 Hz, 1 H), 7.33 (dd, J = 2.2, 8.8 Hz, 1 H), 2.86 (d, J = 13.7 Hz, 2 H), 2.85 (s, 3 H), 2.05 (d, J = 14.1 Hz, 1 H), 1.50 (s, 3 H), 1.44 (d, J = 13.3 Hz, 1 H), 1.36 (d, J = 13.5 Hz, 2 H), 1.33 (s, 6 H); HRMS m/z (M^+) calcd 589.1524, obsd 589.1524.

Imide Amide 11a. To a solution of acid chloride **10c** (0.21 g, 0.49 mmol) and amine **9**[15] (0.15 g, 0.49 mmol) in 30 mL of dry methylene chloride were added a catalytic amount of 4-(dimethylamino)pyridine (ca. 20 mg) and 1.0 mL of triethylamine. The resulting solution was stirred at room temperature for 8 h and was then diluted with 30 mL of methylene chloride, washed with water (3 × 50 mL) and brine (50 mL), dried over $MgSO_4$, filtered, and evaporated to give a tan solid. Flash chromatography on silica gel (5% MeOH in $CHCl_3$) gave 0.28 g (82%) of **11a** as a white powder: mp 176–178 °C; ^{1}H NMR (300 MHz, $CDCl_3$) δ 11.34 (s, 1 H), 8.14 (d, J = 1.5 Hz, 1 H), 7.92 (d, J = 6.3 Hz, 1 H), 7.84 (s, 1 H), 7.71 (dd, J = 1.2, 8.4 Hz, 1 H), 7.67 (s, 1 H), 7.58 (d, J = 9 Hz, 1 H), 7.54 (d, J = 1.8 Hz, 1 H), 7.45 (d, J = 8.7 Hz, 1 H), 7.16 (dd, J = 2.4, 7.2 Hz, 1 H), 6.33 (s, 2 H), 5.77 (d, J = 4.2 Hz, 1 H), 5.29 (dd, J = 4.2, 6.3 Hz, 1 H), 4.97 (dd, J = 3.0, 6.4 Hz, 1 H), 4.51 (dd, J = 3.0, 10.0 Hz, 1 H), 4.25 (m, 1 H), 3.58 (d, J = 14.7 Hz, 1 H), 2.89 (d, J = 13.8 Hz, 2 H), 2.11 (d, J = 13.2 Hz, 1 H), 1.62 (d, J = 14.0 Hz, 1 H), 1.59 (s, 3 H), 1.49 (d, J = 13.8 Hz, 1 H), 1.47 (s, 3 H), 1.37 (s, 2 H), 1.34 (s, 6 H), 1.33 (s, 3 H); HRMS m/z (M^+) calcd 697.2860, obsd 697.2911.

6-*N*-Methyl Imide Ester 11b. Acid chloride **10g** (0.68 g, 1.53 mmol) was converted to amide **11b** as described for the preparation of **11a**. Column chromatography on silica gel (5% MeOH in $CHCl_3$) gave 0.80 g (73%) of **11b**: mp 175–180 °C; ^{1}H NMR (300 MHz, $CDCl_3$) δ 8.35 (s, 1 H), 8.23 (d, J = 6.3 Hz, 1 H), 7.94 (dd, J = 1.4, 8.6 Hz, 1 H), 7.86 (m, 4 H), 7.61 (d, J = 1.9 Hz, 1 H), 7.26 (dd, J = 2.2, 5.0 Hz, 1 H), 5.88 (d, J = 4.3 Hz, 1 H), 5.69 (s, 2 H), 5.39 (dd, J = 1.7, 4.4 Hz, 1 H), 5.03 (dd, J = 2.7, 3.6 Hz, 1 H), 4.59 (d, J = 2.7 Hz, 1 H), 4.35 (m, 1 H), 3.61 (dt, J = 2.3, 14.4 Hz, 1 H), 2.87 (s, 3 H), 2.05 (d, J = 12.5 Hz, 2 H), 2.85 (d, J = 12.0 Hz, 1 H), 1.64 (s, 3 H), 1.46 (s, 3 H), 1.45 (d, J = 12.5 Hz, 1 H), 1.36 (s, 3 H), 1.34 (s, 6 H), 1.31 (d, J = 14.0 Hz, 2 H).

6-Acetoxy-2-naphthoic Acid (12a). A mixture of 10 mL of acetic anhydride, 6-hydroxy-2-naphthoic acid (0.70 g, 3.72 mmol), and 3 mL of pyridine was stirred at room temperature for 2.5 h. The reaction mixture was quenched with water to afford a tan precipitate. The solid was isolated by filtration and washed with 1 N HCl (15 mL) and then with water (ca. 20 mL). The solid was dissolved in CH_2Cl_2 (200 mL), dried over $MgSO_4$, and concentrated to afford 0.80 g (93%) of **12a** as a tan powder: mp 208–210 °C; ^{1}H NMR (300 MHz, $CDCl_3$) δ 8.70 (s, 1 H), 8.13 (dd, J = 1.5, 8.7 Hz, 1 H), 8.01 (d, J = 8.9 Hz, 1 H), 7.88 (d, J = 8.7 Hz, 1 H), 7.63 (d, J = 1.9 Hz, 1 H), 7.33 (dd, J = 2.1, 8.9 Hz, 1 H), 2.38 (s, 3 H).

Methoxymethyl 6-Acetoxy-2-naphthoate (12b). To a solution of acetoxy acid **12a** (0.70 g, 3.0 mmol) in dry THF (15 mL) and triethylamine (1 mL) was slowly added methoxymethyl chloride (0.28 mL, 3.6 mmol). The resulting suspension was stirred at room temperature

for 1 h. The reaction mixture was quenched with ca. 5 mL of cold water, and the solvent was removed by rotary evaporation. The residue was dissolved in EtOAc (50 mL), washed with water (3 × 50 mL) and brine (50 mL), dried over $MgSO_4$, filtered, and evaporated to afford 0.80 g (96%) of **12b** as a brown oil, which solidified upon evacuation: ^{1}H NMR (300 MHz, $CDCl_3$) δ 8.65 (s, 1 H), 8.11 (dd, J = 1.6, 8.7 Hz, 1 H), 7.99 (d, J = 8.9 Hz, 1 H), 7.86 (d, J = 8.6 Hz, 1 H), 7.62 (d, J = 1.6 Hz, 1 H), 7.32 (dd, J = 2.2, 8.9 Hz, 1 H), 5.56 (s, 2 H), 3.60 (s, 3 H), 2.38 (s, 3 H).

Methoxymethyl 6-Hydroxy-2-naphthoate (12c). A solution of acetoxy ester **12b** (0.65 g, 2.37 mmol) in a mixture of 40 mL of MeOH, 7 mL of saturated aqueous $NaHCO_3$, and 7 mL of H_2O was stirred at room temperature for 6 h. The reaction mixture was quenched with 1 N HCl (ca. 10 mL) to afford a tan precipitate. MeOH was removed by rotary evaporation, and the solid was isolated by rapid filtration. The solid was dissolved in EtOAc (50 mL), and the solution was washed with brine, dried over $MgSO_4$, filtered, and concentrated to afford 0.57 g (97%) of **12c** as a tan solid: mp 130-132 °C; ^{1}H NMR (300 MHz, $CDCl_3$) δ 8.58 (s, 1 H), 8.05 (dd, J = 1.6, 8.6 Hz, 1 H), 7.80 (d, J = 8.6 Hz, 1 H), 7.72 (d, J = 8.6 Hz, 1 H), 7.17 (m, 2 H), 5.55 (s, 2 H), 5.49 (s, 1 H), 3.60 (s, 3 H); HRMS m/z [$(M - H)^+$] calcd 231.0657, obsd 231.0658.

Kinetics Studies. The reaction of imide esters **10d** and **10h** with amine **9** in the presence and absence of templates **11a** and **11b** was performed in $CHCl_3$ solution containing ca. 4 equiv of Et_3N. A Waters 600 HPLC equipped with a UV detector (254 nm) was used for the analysis of reaction mixtures. Analyses were performed with a mixture of water-methanol-Et_3N (30:70:0.1) as the mobile phase and a reverse-phase column (Beckman C_{18} column, Ultrasphere ODS dp, 5 μm, 4.6 mm i.d. × 25 cm, flow rate = 1.5 mL/min). The integrations and concentrations of all the peaks were calculated on an NEC computer with Waters 820 Baseline software. In case of prolonged reactions (>100 min), a methanol flush was performed between injections to ensure complete elution of esters **10d** and **10h**. $CHCl_3$ was dried over molecular sieves or by passage through Al_2O_3 before use. All experiments were performed at ambient temperature (21.5-23.0 °C). Each run was performed 2-4 times to obtain average values for the data.

Calibration of HPLC. The HPLC was calibrated by the injection of solutions of amine **9** and template **11a** of varying concentration. A linear relationship between concentration and peak area was observed. Reaction mixtures were analyzed on the basis of either the area of the template peak or the *ratio* of the amine and template peaks.

Reaction Procedures. During initial studies (data presented in Figures 1 and 5), reactions were performed in 100 μL of solvent in 1-mL. Wheaton serum vials equipped with aluminum caps and Teflon-coated silicone septa (procedure A). During subsequent studies (data presented in Figures 2-4), 1-mL Wheaton screw-cap vials equipped with Mininert valves were used to minimize evaporative losses of solvent, and 500 μL of solvent was used to reduce changes in concentration arising from solvent evaporation (procedure B).

Typical Reaction Procedure A. Reaction of Imide Ester 10d and Amine 9. A 1-mL Wheaton serum vial equipped with a aluminum cap and a silicone rubber septum coated with Teflon was charged with 20 μL of $CHCl_3$, ca. 1 μL of Et_3N, 40 μL of amine **9** stock solution (2.05×10^{-2} M), and 40 μL of pentafluoro ester stock solution **10d** (2.05×10^{-2} M). The reaction mixture was shaken gently with a mechanical shaker. Aliquots (1.0 μL) were withdrawn periodically and analyzed by HPLC.

Typical Reaction Procedure B. Reaction of Imide Ester 10d and Amine 9 in the Presence of Template 11a. A 1-mL Wheaton reaction vial equipped with a Mininert valve and a stir vane was charged with 260 μL of $CHCl_3$ and 4.6 μL of Et_3N. Stock solutions of amine **9** (100 μL, 8.2×10^{-2} M), template **11a** (40 μL, 4.1×10^{-2} M), and pentafluoro ester **10d** (100 μL, 8.2×10^{-2} M) were added by a microliter syringe. Aliquots (10 μL) were withdrawn from the reaction solution periodically, diluted with 90 μL of $CHCl_3$, and analyzed by HPLC (10 μL injected).

Acknowledgment. We are grateful to the National Science Foundation for support of this research. J.S.N. thanks the NSF for a postdoctoral fellowship.

Inside-Outside Stereoisomerism. 5. Synthesis and Reactivity of *trans*-Bicyclo[*n*.3.1]alkanones Prepared via the Intramolecular Photocycloaddition of Dioxenones[†,‡]

Jeffrey D. Winkler,*[,1] Bor-Cherng Hong,[2] John P. Hey,[2] and Paul G. Williard[3]

Contribution from the Department of Chemistry, The University of Pennsylvania, Philadelphia, Pennsylvania 19104, Department of Chemistry, The University of Chicago, Chicago, Illinois 60637, and Department of Chemistry, Brown University, Providence, Rhode Island 02912. *Received March 1, 1991. Revised Manuscript Received July 18, 1991*

Abstract: The stereoselectivity of the intramolecular photocycloaddition of a series of bicyclic dioxenones has been examined. The selective formation of trans-fused photoadducts is observed in almost all cases, which upon fragmentation lead to the synthesis of bicycloalkanones with an "inside-outside" or trans intrabridgehead stereochemical relationship. This methodology has been applied to the synthesis of several "inside-outside" bicycloalkanones that cannot otherwise be prepared. The unusual reactivity of both the dioxanone photoadducts and the bicycloalkanone fragmentation products is described.

Introduction

The de Mayo reaction has served as an important example of the utility of enone photocycloaddition chemistry in organic synthesis for almost 30 years. Cycloaddition of the enol of a β-diketone with an alkene leads to the formation of a cyclobutane, which on fragmentation gives a product containing a 1,5-dicarbonyl moiety.[4,5] Since the pioneering studies of Oppolzer[6] and Pattenden,[7] the intramolecular version of this reaction has attracted considerable attention as a powerful method for the construction of structurally complex polycyclic ring systems beginning with readily available starting materials. However, the application of this reaction to the construction of bridged bicyclic

[†] Dedicated to Professor Ronald C. D. Breslow on the occasion of his 60th birthday.

[‡] For the previous paper in this series, see: Winkler, J.; Sridar, V.; Rubo, L.; Hey, J.; Haddad, N. *J. Org. Chem.* **1989**, *54*, 3004.

(1) Address correspondence to this author at the University of Pennsylvania. Recipient of the American Cyanamid Young Faculty Award (1989-1992) and a National Institutes of Health Research Career Development Award (1988-1993). Fellow of the Alfred P. Sloan Foundation (1987-1989).

(2) University of Chicago.

(3) Address correspondence to this author at Brown University regarding the X-ray structural data for **6** and **17**.

(4) de Mayo, P. *Pure Appl. Chem.* **1964**, *9*, 597. de Mayo, P. *Acc. Chem. Res.* **1971**, *4*, 41.

(5) For an excellent recent review of the application of the intramolecular [2 + 2] photocycloaddition reaction in organic synthesis, see: Crimmins, M. *Chem. Rev.* **1988**, *88*, 1453 and references cited therein.

(6) Oppolzer, W. *Acc. Chem. Res.* **1982**, *15*, 135.

0002-7863/91/1513-8839$02.50/0